https://doi.org/10.48048/tis.2025.9130

Antibacterial Effect of an Ethyl Acetate Extract of *Emericella nidulans* Derived from Endophytic Fungus *Rhizophora mucronata* Against Methicillin-Resistant *Staphylococcus aureus*

Nurhadi Nurhadi[1,2], Purwantiningsih Sugita[3,*], Novriyandi Hanif[3], Prasetyawan Yunianto[2], Agus Supriyono[2] and Firdayani[4]

[1]Postgraduate Student of Chemistry Program, Pascasarjana School of IPB University, West Java 16680, Indonesia
[2]Research Center for Pharmaceutical Ingredients and Traditional Medicine, National Research and Innovation Agency (BRIN) Republic of Indonesia, Tangerang Selatan 15314, Indonesia
[3]Department of Chemistry, Faculty of Mathematics and Natural Sciences, Institut Pertanian Bogor, West Java 16880, Indonesia
[4]Research Center for Vaccine and Drugs, Research Organization for Health, National Research and Innovation Agency (BRIN), Tangerang Selatan 15314, Indonesia

([*]Corresponding author's e-mail: purwantiningsih@apps.ipb.ac.id)

Received: 13 October 2024, Revised: 5 November 2024, Accepted: 12 November 2024, Published: 10 January 2025

Abstract

Methicillin-resistant *Staphylococcus aureus* (MRSA) poses a significant global public health challenge due to its resistance to conventional antibiotics, leading to persistent infections, increased healthcare costs, and high mortality rates. MRSA can cause various diseases, including those affecting the skin, subcutaneous tissues, and internal organs. Its resistance is largely driven by the mecA gene, which encodes Penicillin Binding Protein 2a (PBP2a), which prevents β-lactam antibiotics from effectively targeting the bacterial cell wall. In this study, crude extract and fractions of *Emericella nidulans* derived from *Rhizophora mucronata* mangrove were prepared and screened for antibacterial activity against MRSA. *In vitro* tests on ethyl acetate extracts and fractions of *E. nidulans* revealed that they can inhibit MRSA growth in a moderate range. The crude extracts were analyzed using liquid chromatography-high-resolution mass spectrometry (LC-HRMS) to determine the compound contained. Forty-eight compounds were screened through molecular docking analysis to identify the bioactive compounds inhibiting the SauPBP2a receptor. It is indicated that *E. nidulans* shows promise as raw materials for antibacterial against MRSA.

Keywords: *Emericella nidulans*, MRSA, Molecular docking, PBP2a, Bacterial resistance, *Rhizopora mucronata*

Introduction

MRSA is a significant public health concern attributable to its increasing resistance to conventional antibiotics, leading to persistent infections, increased healthcare costs, and high fatality rates linked to infections caused by this organism [1]. MRSA can cause a series of infections that are specific to certain organs, with the most common ones being infections of the pores, skin, and subcutaneous tissue [2]. These infections can then progress to invasive infections such as osteomyelitis [3], meningitis [4], pneumonia [5], lung abscesses, and empyema [6].

MRSA-induced infectious endocarditis is linked to elevated morbidity and mortality rates relative to other pathogens and is associated with intravenous drug misuse [7]. *S. aureus* is the primary etiological agent responsible for foodborne diseases, with an estimated 241,000 cases reported annually in the United States. The estimated yearly incidence rate of MRSA infection ranges from 20 to 50 infections per 100,000 individuals, resulting in a mortality rate of 10 - 30 %. The mortality

rate of this pathogen surpasses the combined mortality rates of AIDS, viral hepatitis, and tuberculosis [8]. Asia has the greatest frequency of MRSA linked to the healthcare industry and the general public globally. The prevalence of MRSA infection is 3.1 % in Indonesia, Java, and Bali, compared to 70 % across Asia [9].

This variant exhibit resistance to β-lactam antibiotics extensively employed for treating *S. aureus* infections. The mecA gene encodes the Penicillin Binding Protein-2a (PBP2a) enzyme, which promotes resistance to MRSA and is not repressed by β-lactam antibiotics [10]. Situated on the staphylococcal cassette chromosome mec (SSCmec), the mecA gene is very transmissible through plasmid transfer. Penicillin and methicillin predominantly function by binding to penicillin-binding protein-2, a protein found in the bacterial cell wall, therefore inhibiting the process of cell wall cross-linking. Consequently, the cell wall becomes weakened, encouraging the ability to destroy bacteria. The mecA gene in MRSA encodes a mutant copy of the PBP2A. Specifically, this mutant protein inhibits the binding of penicillin and cephalosporin to the cell wall [11].

The enzyme PBP2a plays a crucial role as a catalyst in the peptidoglycan crosslinking process during the formation of bacterial cell walls [12]. Consequently, investigating the 3-dimensional structure of the active site of PBP2a in *S. aureus* (SauPBP2a) has been seen as an exciting option for advancing the discovery of specific inhibitors against MRSA [13].

Identifying novel therapeutic agents that can efficiently compete with MRSA is of major significance. Fungal specimens obtained from mangrove *R. mucronata*, especially those with endophytic features, have been identified as a highly promising resource of bioactive substances with antibacterial activities [14]. *E. nidulans*, a fungal species obtained from *R. mucronata*, has been discovered to produce a wide range of bioactive compounds with strong antibacterial properties and contribute significantly to the production of bioactive secondary metabolites. Since its establishment, *E. nidulans* has attracted interest for its extensive collection of natural compounds with strong organic properties. In light of the pressing need for alternatives to existing therapies for resistant bacterial strains, these metabolites offer a promising opportunity for the development of novel antibacterial agents [15].

This research aims to investigate the efficacy of ethyl acetate extract of *E. nidulans* in combating MRSA bacteria. Extraction was performed employing ethyl acetate and subsequently fractionated with solvents or solvent combinations of varying polarity. The extract and its fractions were evaluated for antibacterial efficacy against MRSA *in vitro* utilizing the agar diffusion method. The crude extract underwent chemical analysis by High-Resolution Mass Spectrometry (HRMS). Additionally, the identified compounds were examined *in silico* through molecular docking simulations to ascertain compounds capable of inhibiting the SauPBP2a receptor.

Materials and methods

Material

Endophytic fungus used in this study were isolated from *R. mucronata* mangrove plants taken from the Pantai Indah Kapuk Mangrove Ecotourism Area, Jakarta. The fungal isolates are collected and stored in the BRIN Culture Collection. Preparation of endophytic isolates was conducted using inoculation loop was sterilized by subjecting it to combustion on a Bunsen burner, followed by immersion in ethanol, and finally re-extinguishing after cooling. A pinch of the isolate culture was taken using an inoculation loop. The isolate was then impaled into a petri dish filled with PDA medium and placed in an incubator set at 27 °C for 7 days.

Fermentation

Approximately 1 kg of rice was rinsed and then transferred into a 1,000 mL Erlenmeyer flask, and tightly covered with sterile gauze. The flask is subjected to sterilization by autoclaving at 121 °C for 15 min. It is then stored at ambient temperature in a sterile environment within Laminar Air Flow. Isolates of endophytic fungal that have been cultured in petri dishes are prepared. They are sliced into small segments measuring 1 cm and placed in the rice medium. The prepared samples are placed in a room-temperature incubator for approximately 40 days [16].

Sample preparation and extract fractionation

The solid fermentation results of endophytic fungi were soaked in 1,000 mL of ethyl acetate solvent and left overnight. They were then sonicated for 15 min with several repetitions until the extract became colorless. The filtrate was filtered using filter paper, extracted, and evaporated using a rotary evaporator until a thick extract was obtained. Fractionation of the crude extract was carried out using the vacuum liquid chromatography (VLC) method, employing a stationary phase of silica gel 60 (0.040 - 0.063 mm) and various mobile phases as shown in (**Table 1**).

HRMS analysis

The analysis was conducted using liquid chromatography (Thermo Scientific™ Vanquish™ UHPLC Binary Pump) and Orbitrap high-resolution mass spectrometry (Thermo Scientific™ Q Exactive™ Hybrid Quadrupole-Orbitrap™ High-Resolution Mass Spectrometer). Liquid chromatography utilized an analytical column of Thermo Scientific™ Accucore™ Phenyl-Hexyl (100 mm×2.1 mm ID×2.6 µm). The mobile phases consisted of MS-grade water containing 0.1 % formic acid (A) and MS-grade acetonitrile containing 0.1 % formic acid (B) employing gradient technique with flow rate of 0.3 mL/min. First, the mobile phase B was set at 5 % and increased gradually to 90 % in 16 min. Then, it held at 90 % for 4 min and continued to the initial condition (5 % B) until 25 min. The column temperature was set to 40 °C, and the injection volume was 3 µL. Full MS/dd-MS2 acquisition mode was used for the untargeted screening at either positive or negative ionization polarities/states. Sheath, auxiliary, and sweep gases were all nitrogen, with arbitrary units (AU) of 32, 8, and 4, respectively.

The capillary temperature was set at 320 °C, the auxiliary gas heater temperature was set at 30 °C, and the spray voltage was 3.30 kV. The resolution employed was 70,000 for full MS and 17,500 for dd-MS2, both in positive and negative ionization modes, and the scan range was 66.7 - 1,000 m/z. XCalibur 4.4 software (Thermo Scientific, Bremen, Germany) controlled the machine. Using Thermo Scientific Pierce ESI ion calibration solutions (Waltham, MA), the instrument was tuned and calibrated once a week in both ESI positive and negative modes to guarantee optimal and reliable instrumental performances throughout the analysis in terms of mass accuracy (< 5 ppm), ion transfer, ion isolation, and instrumental sensitivity. Software called Compound Discoverer® (Thermo Scientific, USA) was used to evaluate HRMS data. After raw data analysis, the results were filtered by name, MS2 for DDA for preferred ion, and best matched to MzCloud. The analytical method follows reference 17 by modifying the mobile phase from methanol to acetonitrile [17].

Antibacterial test

The MRSA clinical bacteria utilized in the antibacterial activity test were acquired from the microbiology laboratory of M. Djamil General Hospital Padang. The antibacterial test culture preparations were cultivated on Mueller Hinton broth at 37 °C for 24 h. Turbidity was determined by calibrating to 0.5 McFarland standards (1×10^8) colony-forming units per millilitre. The efficacy against bacterial growth was assessed on Muller Hinton agar plates coated with MRSA bacterial culture. Paper discs dripped with samples were attached to the agar medium.

The test samples for each were prepared at a concentration of 25 mg/mL following the Bauer-Kirby test method (DIN 59040) as described by Kjer *et al.* [16]. The extracts and crude fractions were dissolved in methanol. Susceptibility discs were dripped with 20 µL of the test solution prepared for each test solution, and allowed to evaporate. Chloramphenicol at 1 mg/mL was used as the positive control, and the solvent (methanol) as the negative control. The plates were incubated at 37 °C for 18 h [18].

Molecular docking

We conducted molecular docking using Molegro Virtual Docker (MVD) 6.0, a licensed software version 2013.6.0.0 to 2013.05-21. We selected a suitable target protein from the Protein Data Bank (PDB) and obtained the 3D structure of the target protein PBP2a from the public domain database (PDB ID: 1MWT) available at https://rcsb.org. We removed water and cofactors from the MRSA protein and then extracted an attached ligand from the protein. Subsequently, we docked the ligand back into the protein by optimizing the x, y, and z coordinates and radius. We performed a docking procedure and recorded the Root Mean Square

Deviation (RMSD) value. It is important to note that RMSD values should be less than or equal to two.

The structure of the ligands (compounds derived from HRMS analysis of crude ethyl acetate extract) was drawn and minimized using ChemDraw 18.1.2.18 software. The structures were stored in the mol2 file data format. The subsequent procedure involved docking each ligand to the 1MWT receptor in the validated binding site. The docking procedure was iterated 10 times. Docking scores, hydrogen bonds, hydrophobic interactions, and visualization of ligand and target protein binding were conducted using MVD and ligplot modelling. Reanalysis of the ligand test results with the highest scores (rerank) was conducted using the Lipinksi rule on the website http://www.scfbio-iitd.res.in/software/drugdesign/lipinski.jsp. The active chemical underwent toxicity testing performed using the website https://tox.charite.de/protox3/index.php?site=compound_input.

Results and discussion

Identification of endophytic fungus isolate

The isolates that grew were identified macroscopically (**Figure 1(A)**) and microscopically (**Figure 1(B)**). The results of PCR identification carried out by Abraham *et al.* [19] on endophytic fungal isolates showed that this endophytic fungus is the species *E. nidulans*.

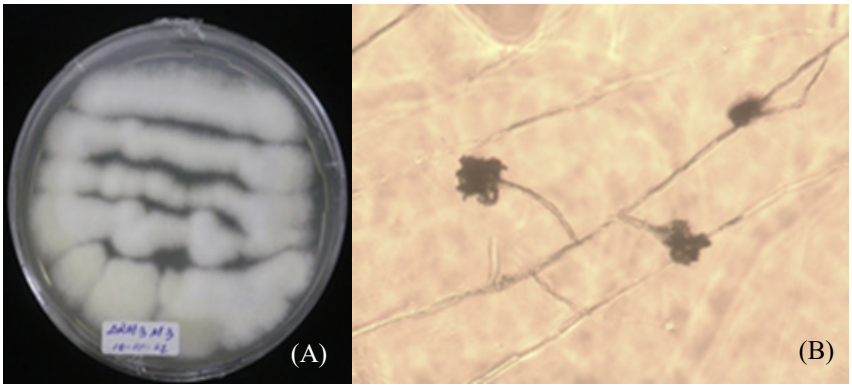

Figure 1 Isolate *E. nidulans*: (A) Macroscopically and (B) Microscopically.

In order to produce more potent antibacterial secondary metabolites from endophytic fungi compared to other planting media, a fermentation process was carried out using rice media and ethyl acetate as an extraction solvent [14]. From 1 kg of rice fermented with endophytic fungus for 40 days, the solids were extracted using ethyl acetate, yielding approximately 2 - 3 g. It is suggested that the extract could contain non-polar to moderately polar compounds, such as alkaloids, flavonoids, or phenolic compounds. The crude extract was then fractionated using the VLC method to obtain 9 fractions are shown in (**Table 1**).

In the extraction of secondary metabolites from natural sources, fractionation is an essential procedure that involves separating the crude extract into many fractions. The incorporation of solvents with varying polarity in fractionation improves the separation process by allowing separation of substances based on their solubility characteristics, therefore improving the purity of the desired residue. Fractionation is the process of dissolving the crude extract into various fractions, which simplifies and facilitates following purification procedures. This, in turn, facilitates the identification and characterization of the separated compounds. The study used solvents in VLC, including toluene, dichloromethane, acetone, methanol, and the combinations. The solvent polarity, which progresses from nonpolar to polar [20], affects the elution of components. Polar solvents are more efficient in eluting polar analytes and have greater solvent strength. The chromatography process's velocity is also influenced by the solvent's polarity. This study modified solvents to maximize separation conditions.

LC-HRMS spectral analysis

Liquid chromatography high-resolution mass spectrometry (LC-HRMS) was utilized to quantify the mass-to-charge ratio (m/z) of ions in fungal ethyl acetate extract. It accurately measures molecular weights and identifies complex compounds, even in complex samples with hundreds of substances [21,22]. The chromatogram profile in high-performance liquid chromatography (HPLC) or ultra-high-performance liquid chromatography (UHPLC) depends on the polarity of the compounds being separated. The mobile phase A is polar, while the stationary phase B is less polar. The stationary phase is often C18, which is nonpolar, so more nonpolar compounds will interact more strongly with it. Polar compounds elute faster, exiting the column earlier, while nonpolar compounds have longer retention. The elution gradient profile starts with a higher proportion of water (phase A) and gradually increases the proportion of acetonitrile (phase B), forcing more nonpolar compounds out of the column.

Thermo Scientific™ Accucore™ Phenyl-Hexyl column is a reversed-phase column with unique properties, including polar and aromatic phenyl groups and nonpolar hexyl groups attached to silica particles. The column is generally nonpolar due to its hydrophobic interactions, but has a different selectivity character towards aromatic compounds or those with certain polar groups. In conclusion, the Accucore™ Phenyl-Hexyl column is a nonpolar column with added selectivity towards aromatic compounds. Based on HRMS results, more than 400 compounds were identified from the extract. These compounds were then re-sorted according to their compatibility with the literature. The compounds were selected as the best match for MzCloud, with a probability of over 90 % and a delta mass value of under 5 ppm. In all, 47 compounds were obtained from the sorting results.

The identified compounds can be categorized into primary metabolites, secondary metabolites, and other compounds, which are included in the primary metabolite group, are also found in organisms, plants, fungi other than the *E. nidulans* species according to the attached references, including: 16-hydroxyhexadecanoic acid (fatty acids) [23], 2'-*O*-methyladenosine (nucleosides) [24], 6-hydroxynicotinic acid (carboxylic acids) [25], adenine (purines) [26], adenosine (nucleosides) [27], betaine (quaternary ammonium compounds) [28,29], choline (quaternary ammonium compounds) [30], ethyl oleate (fatty acid esters) [31], gluconic acid (carboxylic acids) [32], hypoxanthine (purines), L(-)-carnitine (amino acids and derivatives) [33], L-phenylalanine (amino acids) [34], methyl palmitate (fatty acid methyl esters) [35], monoolein (glycerolipids) [36], nicotinic acid (vitamins) [37], 1-linoleoyl glycerol (glycerolipids) [37-39] palmitic acid (fatty acids), α-linolenic acid (fatty acids) [37,40,41], uracil (pyrimidines) [42,43]. Meanwhile, those included in the secondary metabolite group include: (-)-caryophyllene oxide (terpenoids) [44,45]; 2,3,5,6-tetramethylpyrazine (pyrazines) [46], 9-oxo-10(E),12(E)-octadecadienoic acid (oxo fatty acids) [47], agroclavine (alkaloids) [48], citral (terpenoids) [49], cordycepin (nucleoside analogs) [50], oleamide (fatty acid amides) [51].

There are also other groups of compounds such as bis(3,5,5-trimethylhexyl) phthalate which is classified as a phthalate ester, Bis(4-ethylbenzylidene) sorbitol is included in the sorbitol derivative group), Bis(7-methyloctyl) adipate) is included in the adipate ester group and several other compounds. Indications of synthetic compounds as mentioned are possible. According to the study (Yadav *et al.* [52]) pollutant particles such as dust, heavy metals, and other hazardous chemical compounds can be captured by the leaves and roots of mangrove trees. In addition, the location of the mangrove plants used as samples is in the center of the capital city in Jakarta where there is a population density and there are various sectors such as office centers, business, trade, recreation, tourism, housing, schools, and others where there is industrial and household waste. The total ion chromatogram of HRMS analysis of crude extract of ethyl acetate is shown in (**Figure 2**). The data has been attached in the supplementary (**Tabel (S1)**).

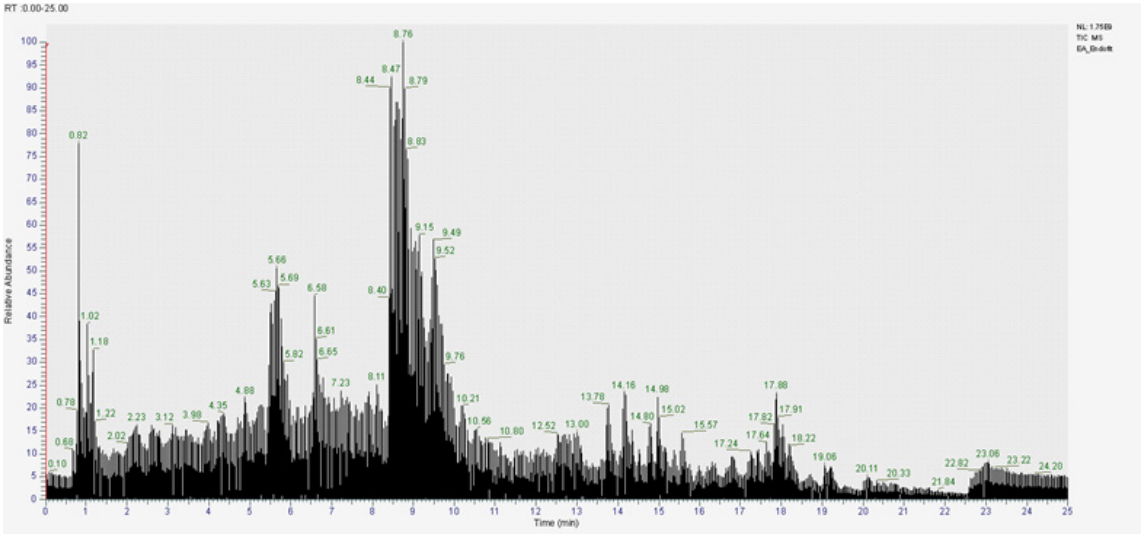

Figure 2 The total ion chromatogram of crude extract of ethyl acetate from *E. nidulans*.

***In vitro* antibacterial activity of ethyl acetate extract of *Emiricella nidulans* fungus**

The antibacterial activity of ethyl acetate extract of *E. nidulans* fungus obtained from *R. mucronata* mangrove plant was tested against MRSA test bacteria in samples with a concentration of 25 mg/mL. The inhibition zone of each sample tested was as follows, crude extract (7.31 mm ± 0.217), fraction-4 (9.62 mm ± 0.077), fraction-6 (8.69 mm ± 0.263), fraction-7 (8.01 mm ± 0.299), fraction 8 (7.36 mm ± 0.136), fraction 9 (7.62 mm ± 0.164) while the positive control using chloramphenicol with a concentration of 1 mg/mL had an inhibition zone of 19.61 mm ± 0.304. Figures of the antibacterial activity of crude ethyl acetate extract, fractions, positive, and negative control using agar disc diffusion method and zone of inhibition are shown in (**Table 1**) supplementary (**Table (S2)**) and (**Figure 3**).

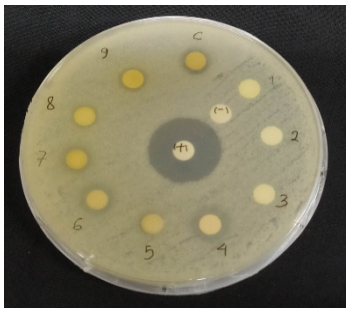

Figure 3 Antibacterial activity of crude extract and ethyl acetate fractions, positive, negative controls using agar disc diffusion method against MRSA bacteria.

Tabel 1 Inhibition zone of crude extract and ethyl acetate fractions, positive, negative controls using agar disc diffusion method against MRSA bacteria.

Code	Name	Description	Inhibition Zone (mm)
C	crude extract	ethyl acetate	7.31 ± 0.217
1	fraction-1	toluene 100	-
2	fraction-2	toluene-dichloromethane (50:50)	-
3	fraction-3	toluene-dichloromethane (20:80)	-
4	fraction-4	dichloromethane-acetone (95:5)	9.62 ± 0.077
5	fraction-5	dichloromethane-acetone (80:20)	-

Code	Name	Description	Inhibition Zone (mm)
6	fraction-6	dichloromethane-acetone (60:40)	8.69 ± 0.263
7	fraction-7	dichloromethane-acetone (40:60)	8.01 ± 0.299
8	fraction-8	acetone 100	7.36 ± 0.136
9	fraction-9	methanol 100	7.62 ± 0.164
(+)	positive control	chloramphenicol	19.61 ± 0.304
(–)	negative control	methanol 100	-

The analysis of MRSA antibacterial activity reveals that both the crude ethyl acetate extract and its corresponding fraction exhibit moderate activity. However, the extract has a lower average inhibition zone (7.31 mm ± 0.217) compared to the average fractionation results, particularly for fraction-4, fraction-6, fraction-7, fraction-8, and fraction-9, which have inhibition zones of 9.62 ± 0.077, 8.69 ± 0.263, 8.01 ± 0.299, 7.36 ± 0.136, and 7.62 ± 0.164, respectively. We classify the inhibition zone measurement results based on their strength: very strong (20 - 30 mm), strong (10 - 20 mm), moderate (5 - 10 mm), and weak (5 mm) [53]. The crude ethyl acetate extract exhibits a lower inhibition zone compared to its fractions, likely due to the presence of numerous compounds in the extract. The quantity of compounds that contribute to anti-MRSA activity is relatively small compared to those that lack inhibitory activity. The fractions of chemical compounds have started to concentrate, resulting in an inhibition zone that is larger than that of the crude extract. As a positive control, researchers have used chloramphenicol, a pure compound with a larger inhibition zone than the crude extract and its fractions.

Pure active compounds only consist of components that directly play a role in antibacterial activity, while the extract contains other compounds that may not have an antibacterial effect and can even reduce the effectiveness of the active compound [54]. Methanol, which is a solvent for testing samples, does not affect the inhibition.

Computational prediction of molecular docking

We validated the method by extracting the native ligand (Open Form-Penicillin G) and then performing the redocking operation. If the resulting RMSD value is less than 2, the docking simulation is considered valid. The native ligand validation using the MVD application indicates that the receptor binding site is located at coordinates x = –36.94, y = 45.93, z = 66.80, with a radius of 15. Redocking yields a binding energy of –87.0279 kcal/mol for the native ligand, with an RMSD of 0.93474. Re-docking yields a satisfactory pose when it closely aligns with the initial pose of the native ligand (**Figure 4**) supplementary (**Table (S3)**).

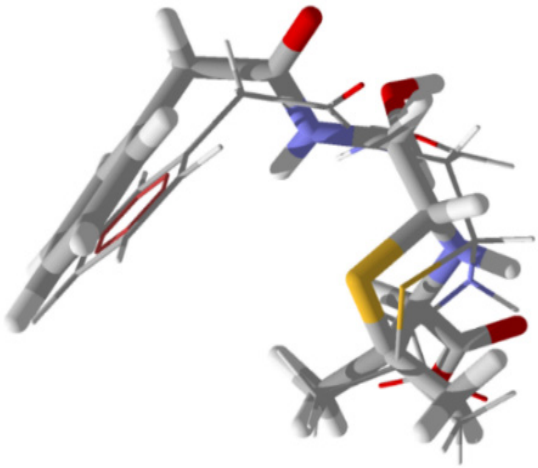

Figure 4 Comparison of native ligand (wireframe) with redocking result simulation (stick).

A total of 47 compounds including native ligands were docked to the PBP2a protein, where each ligand was determined to have the best position indicated by the docking score (rerank). The rerank score value of the docking result is assumed to be the free energy of binding between the target protein receptor and the inhibitory ligand. A more negative value indicates that the ligand-protein binding is more stable, which means that the interaction between the protein and the ligand can inhibit the performance of the PBP2a protein receptor. The rerank docking score for each ligand-protein binding affinity from highest to lowest are shown in **Figure 5**.

Based on the results of virtual screening, 9 test ligands were obtained which had better binding values compared to the native ligand, while the natural ligand was still better than the commercial drug (chloramphenicol). Molecular docking simulations were conducted to identify the chemicals responsible for the antibacterial activity of this fungus. It facilitates the prediction of molecular interactions between a protein and a ligand at the cavity locations. Extracts derive their pharmacological properties from their bioactive components. These chemicals interact with specific functional proteins (such as receptors) that may activate or inhibit them. Docking analysis was conducted to evaluate the lowest energy and interactions, including the formation of hydrogen bonds inside the complex. In this study, molecular docking simulation was conducted PBP2a. PBP2a is an important factor in MRSA resistance. PBP2a facilitates cell wall production in the presence of most β-lactams. Focusing on PBP2a presents a significant opportunity for addressing the MRSA menace [55].

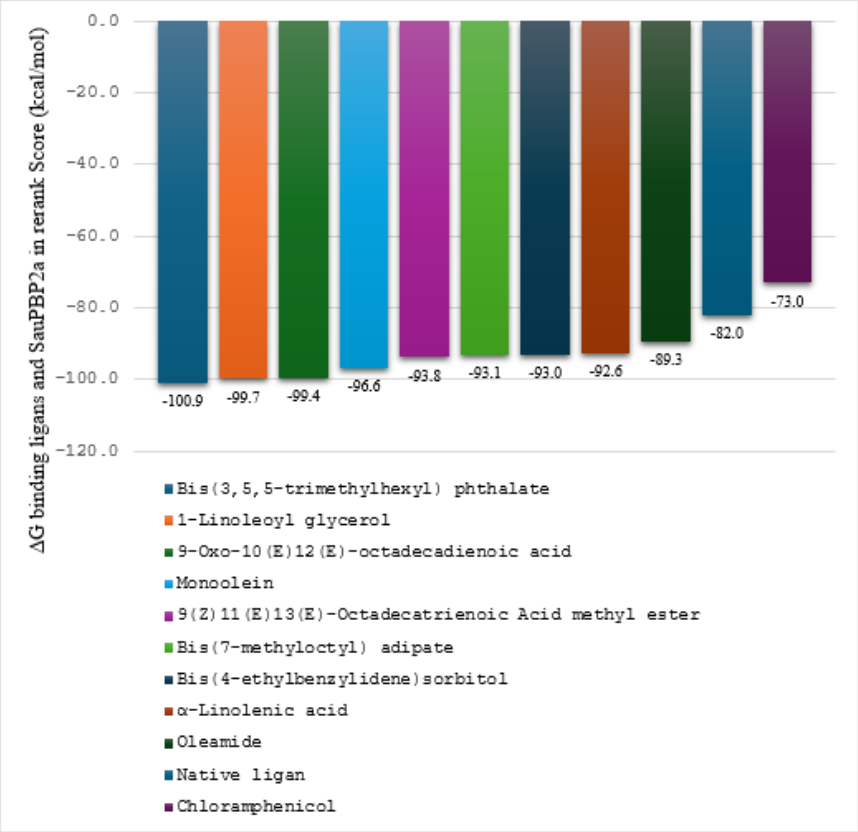

Figure 5 Rerank score for each ligand-protein binding affinity.

Prediction of bioavailability and toxicity of test ligands

Table 2 presents a summary of Lipinski analysis on selected ligands that exhibit more effective binding affinity compared to the native ligand. The chosen ligands were further assessed for their toxicity using the following parameters: Hepatotoxicity, carcinogenicity, oral toxicity, and immunotoxicity. The obtained analysis results are presented in **Table 3**.

Table 2 Lipinsky parameter of selected ligands.

No	Name	MW	Log P	HBD	HBA	Molar refractivity
1	Open Form-Penicillin G	336.41	0.81	3	6	88.16
2	Bis (3,5,5-trimethylhexyl) phthalate	418.61	6.93	0	4	122.71
3	1-Linoleoyl glycerol	354.52	4.70	2	4	103.41
4	9-Oxo-10(E)12(E)-octadecadienoic acid	294.43	5.06	1	3	87.38
5	Monoolein	356.54	4.92	2	4	103.50
6	9(Z)11(E)13(E)-Octadecatrienoic Acid methyl ester	292.46	5.75	0	2	91.28
7	Bis (7-methyloctyl) adipate	398.62	6.85	0	4	116.23
8	Bis (4-ethylbenzylidene) sorbitol	414.49	3.06	2	6	110.79
9	a-Linolenic acid	278.43	5.66	1	2	86.90
10	Oleamide	281.48	6.56	2	2	89.81

Note: MW = Molecular weight, HBD = Hydrogen bond donors, HBA = Hydrogen bond acceptors, Yellow colour = It does not meet Lipinski's requirements.

The Lipinski's analytical criteria state that a molecule should have a molecular mass of fewer than 500 Daltons, a high lipophilicity with a LogP value below 5, fewer than 5 hydrogen bond donors, fewer than 10 hydrogen bond acceptors, and a molar refractivity range from 40 to 130. Several test ligands meet the Lipinski's rule of 5 requirements, such as ligand 1-linoleoyl glycerol, monoolein, and, Bis(4-ethylbenzylidene) sorbitol. Other ligands do not meet the criteria because their LogP values are higher than 5. Ligands that do not dissolve well in water but do well in fat (higher positive LogP) will have lower bioavailability. Moreover, adipose tissues will sequester it, making its plasma levels unsustainable. This will then change the drug's effectiveness (though a medicine with high *in vitro* potency might not be helpful) and its excretion, making it more harmful to the whole body [56].

Table 3 Results of toxicity prediction analysis of test ligands and native ligands.

No	Name	HP	CA	IM	Class	LD_{50} (mg/kg)
1	Open form penicillin G	–	–	–	3	1,000
2	Bis(3,5,5-trimethylhexyl) phthalate	–	+	–	6	10,000
3	1-Linoleoyl glycerol	–	–	–	6	39,800
4	9-Oxo-10(E)12(E)-octadecadienoic acid	–	–	–	5	3,200
5	Monoolein	–	–	–	6	39,800
6	9(Z)11(E)13(E)-Octadecatrienoic Acid methyl ester	–	–	–	5	5,000
7	Bis(7-methyloctyl) adipate	–	+	–	5	5,000
8	Bis(4-ethylbenzylidene)sorbitol	–	–	–	5	4,000
9	a-Linolenic acid	–	–	–	6	10,000
10	Oleamide	–	–	–	6	11,730

Note: HP = Hepatoxicity, CA = Carcinogenicity, IM = Immunotoxicity, (–) = Inactive (+) = Active.

Based on the toxicity prediction analysis of the test ligands, none of the test ligands exhibit evidence of liver toxicity. Therefore, all test ligands are deemed safe in terms of their potential toxicity to the liver. In the carcinogenicity test, it is anticipated that 2 test ligands, specifically bis(3,5,5-trimethylhexyl) phthalate (**2**) and Bis(7-methyloctyl) adipate (**7**), may exhibit carcinogenic efficacy in the human body. Substances known as carcinogens can stimulate the development of both benign and malignant cancer cells. Within the immunotoxicity prediction study, no test ligands were shown to be prospective agents capable of causing detrimental effects on both local and systemic immune function. The acute toxicity test indicates that all the ligands evaluated are expected to be safe and may be considered as potential medication candidates as they belong to toxicity prediction classes 5 and 6.

According to Gadaleta *et al.* [57], the LD50 can be categorized into 6 classes: Class 1 (very toxic), class 2 (highly toxic), class 3 (toxic), class 4 (somewhat toxic), class 5 (non-toxic), and class 6 (safe). Acute toxicity is typically referred to as LD_{50} [58], where LD stands for lethal dosage fatal amount and the subscript 50 indicates that 50 % of the animals given the chemical under carefully monitored laboratory circumstances will die from the dose. To put it another way, LD_{50} is the statistically determined amount of a drug that, when given to a population of test animals by oral, cutaneous, inhalation, or intravenous routes, results in 50 % of the animals dying. This test's determination looks at the connection between dosage and the most severe reaction, which is death. The LD_{50} and the dose required to cause death decrease with increasing toxicity or potency of the substance. Therefore, an oral LD_{50} of 500 mg/kg of a drug would be much less hazardous than a drug with an LD_{50} of 5 mg/kg. Typically, milligrams of substance per kilogram of animal body weight (mg/kg bb) is how the LD_{50} is expressed. This provides details about the health risks that can occur from short exposures.

The toluene-dichloromethane fraction of the ethyl acetate extract comprises nonpolar to semi-polar molecules attributable to their nonpolar or slightly polar solvents. To estimate the LogP (octanol-water partition coefficient), evaluate the compounds' lipophilicity. Soluble in a toluene and dichloromethane mixture generally exhibit a high LogP, whereas nonpolar or semi-polar molecules possess a LogP ranging from 3 to 6, contingent upon the molecular size and the presence of functional groups. An overview of the analysis of the results of Ligand-protein interactions, including hydrogen bonds and hydrophobic interactions is presented in (**Table 4**) supplementary (**Table (S4)**). (**Figure 6**) displays 7 test ligands exhibiting superior values compared to the native ligand in 2 dimensions using LigPlot+.

The open form of penicillin, as a native ligand (1), is associated with a total of 4 amino acid interactions: Hydrogen bonds with Ser462, Ser598, Thr600, and Ser403, and hydrophobic interactions with Tyr519, Gly599, Gly402, Ala642, Tyr446, and Gln613. Hydrogen bonds contribute to the resilience of protein structures and impart the specificity necessary for macromolecular interactions, whereas hydrophobic interactions play a role as well. **Figure 6** illustrates the 2D depiction of the binding of the native ligand and the test ligand to the receptor. Interactions are crucial for preserving the conformation of ligand-receptor bonds; when both bonds are present, the resulting interaction can be characterized as robust. Fourteen critical residues have been identified in the active site of PBP2a, namely Ser337, Lys340, Ser403, Lys406, Tyr446, Ser462, Asn464, Thr500, Ser548, Gly549, Ser598, Gly599, Thr600, and Met681. These amino acids serve as receptor sites for docking analysis aimed at identifying potential inhibitors of the SauPBP2a active site [59].

The evaluation of molecular docking simulations indicated that ligand 1-linoleoyl glycerol (**3**) associates with PBP2a, exhibiting a rerank score of –99.7437 kcal/mol. Two hydroxyl groups on the ligand demonstrate hydrogen bonds with amino acid residues Ser598 at a bond length of 2.14 Å and His583 at a bond length of 2.6 Å, while the hydrophobic contact with amino acid residue Ala642. The ligand 9-Oxo-10(E),12(E)-octadecadienoic acid (**4**), with a rerank score of –99.4385 kcal/mol, interacts with PBP2a via hydrogen bonding. The ketone functional group on the ligand acts as a proton acceptor, binding to amino acid residues Ser462 at a bond length of 2.77 Å and Ser403 at a bond length of 2.76 Å. Conversely, the hydroxyl functional group on the carboxylic acid serves as a proton donor, interacting with amino acid residue

Ser643 at bond lengths of 2.62 and 2.69 Å, and with amino acid residue Gly640 at a bond length of 2.60 Å. Comparative analysis of hydrogen bonding and hydrophobic interactions with amino acid residues Ser462, Ser403, and Tyr446.

The monoolein ligand (**5**), exhibiting a rerank score of –96.5963 Kcal/mol, interacts with PBP2a via hydrogen bonds from two hydroxyl groups. The 1st hydroxyl group is bound to Gly 640 with a bond length of 2.60 Å and to Ser 643 with bond lengths of 2.62 and 2.69 Å. The 2nd hydroxyl group interacts with Ser 403 at a bond length of 2.67 Å and with Ser 462 at a bond length of 2.77 Å. The 9(Z),11(E),13(E)-Octadecatrienoic acid methyl ester ligand (**6**), with a rerank score of –93.7813 kcal/mol, creates hydrogen bonds through its ester group, acting as a proton acceptor that interacts with the amino acid residue Tyr441 at a bond length of 2.93 Å. This ligand exhibits similarities in binding to the native ligand solely through hydrophobic interactions at the amino acid residues Try446 and Try519.

Table 4 The analysis of the results of Ligand-protein interactions.

No	Compound name	Molecular formula	Rerank score (kcal/mol)	H bond length Å	H bond interaction	Hydrophobic interaction
1	Ligan native open form -penicillin G	$C_{16}H_{20}N_2O_4S$	–87.0279	3.15 2.64 2.9 2.53 2.65 2.69	Ser462 Ser598 Thr600 Ser403 Ser403 Asn464	Tyr 519, Gly599, Gly402, Ala642, Tyr446, Gln613.
2	Bis(3,5,5-trimethylhexyl) phthalate			2.64 2.9 2.53	Ser598 Thr600 Ser403	Thr582, Glu447, Ala642, Ser598, Gly599, Thr600, Glu521, Glu602, Asn464, Try446, His583.
3	1-Linoleoyl glycerol			2.65 2.69	Ser403 Asn464	Val448, Ser643, Glu447, Met641, Ala642, Thr600, Ser462, Ser461, Ile459, Val578, Glu460, Thr582, Tyr446.
4	9-Oxo-10(E)12(E)-octadecadienoic acid	$C_{18}H_{30}O_3$	–99.4385	2.77 2.67 2.60 2.62	Ser462 Ser403 Gly640 Ser643	His583, Met641, Tyr446, Ser461, Thr600, Glu602, Tyr519, Gln521, Thr444, Asn464, Ala462.
5	Monoolein	$C_{21}H_{40}O_4$	–96.5963	2.69 2.65 3.17 2.87 2.97 3.09	Ser643 Gly640 Ala642 Tyr446 Ser643 Ser643	His583, Met641, Gln521, Thr444, Tyr441, Asn442, Tyr519, Glu602, Asn464, Thr600, Ser403, Ser462.
6	9(Z)11(E)13(E)-Octadecatrienoic acid methyl ester	$C_{19}H_{32}O_2$	–93.7813	2.93	Try 441	His583, Thr582, Ser462, Ser461, Glu447, Tyr446, Ser598, Thr600, Gln521, Tyr519, Ser403, Asn464, Thr444, Asn442.
7	Bis(7-methyloctyl) adipate	$C_{24}H_{46}O_4$	–93.0731	2.66	Ser598	Ala642, Gly599, His583, Met641, Tyr446, Thr582, Thr600, Gln613, Glu602, Gln521, Ala601, Ser643, Asn464, Arg445, Asp586, Ser462, Ser403.
8	Bis(4-ethyl-benzylidene) sorbitol	$C_{24}H_{30}O_6$	–93.0372	3.10 2.75 2.53 2.69	Thr600 Ser403 Ser403 Asn464	Glu460, Thr582, Ser461, Ser462, Ser598, His583, Tyr446, Arg445, Thr444, Gly402, Asp516, Ala601, Glu602, Gln521, Tyr519, Tyr441.

No	Compound name	Molecular formula	Rerank score (kcal/mol)	H bond length Å	H bond interaction	Hydrophobic interaction
9	α-Linolenic acid	$C_{18}H_{30}O_2$	–92.6499			Ser643, Ala642, His583, Thr582, Tyr446, Glu460, Ser461, Ser598, Ser462, Ser403, Thr600, Gly599, Met641, Glu447.
10	Oleamide	$C_{18}H_{35}NO$	–89.305	2.29 3.25 2.79	Ser598 Lys597 Ile459	Met641, Thr582, His583, Ala642, Ser461, Glu460, Ser462, Val578, Thr600, Tyr446, Gly599, Syr403, Asn464.

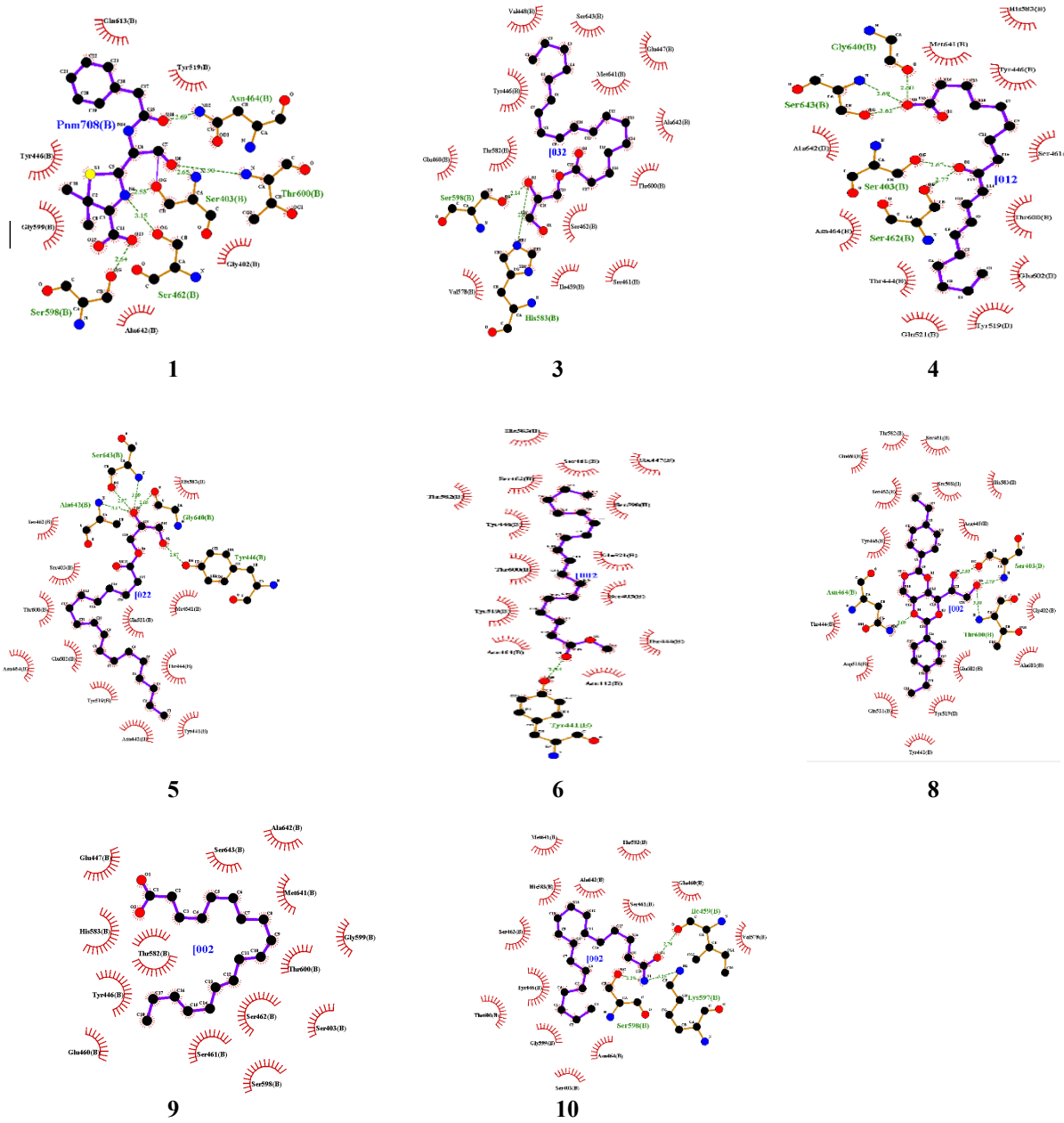

Figure 6 Seven test ligands exhibiting superior values compared to the native ligand in two dimensions using LigPlot+.

Bis(4-ethylbenzylidene)sorbitol (**8**) ligand exhibiting a rerank score of –93.0372 kcal/mol. Hydrogen bond interactions transpire with the amino acid residue Ser403 at the OH functional group, exhibiting bond lengths of 2.53 and 2.75 Å. Additional hydrogen contacts are observed with the amino acid residue Thr600, presenting a bond length of 3.10 Å, and with the amino acid residue Asn464, which has a bond length of 2.69 Å. Similarity of hydrophobic interactions with natural ligands at residues Tyr466, Tyr519, and Gly402. This ligand exhibits the greatest binding site resemblance to native ligands in comparison to other test ligands. α-Linolenic acid (**9**) ligand exhibiting a rerank score of –92.6499 kcal/mol. This ligand exhibits no hydrogen interactions; it only demonstrates hydrophobic interactions with the PBP2a protein. The oleamide (**10**) ligand exhibits a rerank score of –89.305 kcal/mol and interacts with the PBP2a protein via hydrogen bonds formed by the NH functional group, which has a bond length of 2.29 Å, binding to the amino acid residues Ser598 and Lys597 at a bond length of 3.25 Å. Additionally, the hydroxyl functional group binds to the amino acid residue Ile459 with a bond length of 2.79 Å. The resemblance of hydrophobic interactions with natural ligands in the amino acid residues Ala642, Tyr446, and Gly599.

There are two compounds identified as plastic compounds in the crude extract, the 1st is bis(3,5,5-trimethylhexyl) phthalate (**2**) and the 2nd is bis(7-methyloctyl) adipate (**7**) which is a potential carcinogen. There is a possibility that Phthalate compounds, known as plasticizers, are absorbed and accumulated by mangrove plants from the surrounding environment. Information regarding the presence of plastic compounds in mangrove plant extracts is also in a study conducted by Uddin *et al.* [60] who isolated the compound 2"-(methoxycarbonyl)-5"-methylpentyl 2'-methylhexyl phthalate found in mangrove fern, as well as studies (Pontes *et al.* [61] and Victório *et al.* [62]), which identified the presence of plastic compounds in mangrove plants. None of Bis(3,5,5-trimethylhexyl) phthalate and Bis(7-methyloctyl) adipate compounds can cause liver damage or immune system damage. The active constituents, the bis(3,5,5-trimethylhexyl) phthalate (**2**) and bis(7-methyloctyl) adipate (**7**), are predicted to be potential carcinogens based on ADMET analysis. This analysis indicates the need for proper consideration and further investigation into the safety and potential health implications associated with the consumption of these extracts.

Several potential compounds from this study have been reported to have antibacterial activity, including 9-oxo-10(E),12(E)-octadecadienoic acid (**4**) compounds which have been reported to increase antibacterial activity [63], Oleamide (**10**) is suspected to have antibacterial activity [64], α-Linolenic acid (**9**) shows antibacterial activity [65]. It is suspected that the presence of nonpolar active fatty acid compounds allows for better activity than other fractions against MRSA bacteria in the antibacterial activity test in fraction-4. In fact, fatty acid and monoglyceride compounds are promising antibacterial agents [66].

The present work is a contribution to the guide on the isolation of active compounds in *E. nidulans* against MRSA. Compounds exhibiting the most unfavorable docking scores and ADMET features that satisfy pharmacological criteria can be advanced as markers of active antibacterial agents. To confirm the computational results, more bioassay-guided experiments for isolates or pure compounds are required.

Conclusions

Ethyl acetate extract of *E. nidulans* showed antibacterial activity against MRSA *in vitro* and contained 47 compounds based on LC-HRMS analysis. *In silico* studies predict that nine compounds such as 1-linoleoyl glycerol, 9-oxo-10(E)12(E)-octadecadienoate, monoolein, methyl ester of 9(Z),11(E),13(E)-octadecadienoate, bis(4-ethylbenzylidene) sorbitol, α-linolenic acid, and oleamide have the ability to inhibit the SauPBP2a receptor.

Acknowledgements

This work was supported by National Research and Innovation Agency (BRIN) Indonesia through Program Riset dan Inovasi untuk Indonesia Maju (RIIM) 2nd Term of 2022.

References

[1] P Nandhini, PK Gupta, AK Mahapatra, AP Das, SM Agarwal, S Mickymaray, A Alothaim and M

Rajan. *In-silico* molecular screening of natural compounds as a potential therapeutic inhibitor for Methicillin-resistant *Staphylococcus aureus* inhibition. *Chemico-Biological Interactions* 2023; **374**, 110383.

[2] PY Ong. Recurrent MRSA skin infections in atopic dermatitis. *The Journal of Allergy and Clinical Immunology: In Practice* 2014; **2(4)**, 396-399.

[3] KL Urish and JE Cassat. *Staphylococcus aureus* osteomyelitis: Bone, bugs, and surgery. *Infection and Immunity* 2020; **88(7)**, e00932-19.

[4] WD Longhurst and JM Sheele. Spontaneous methicillin-resistant *Staphylococcus aureus* (MRSA) meningitis. *The American Journal of Emergency Medicine* 2018; **36(5)**, 909.

[5] KZ Vardakas, DK Matthaiou and ME Falagas. Incidence, characteristics and outcomes of patients with severe community acquired-MRSA pneumonia. *European Respiratory Journal* 2009; **34(5)**, 1148-1158.

[6] AD Lewis, MR Bridwell, MD Hambuchen, TB Clay and KW Orwig. Correlation of MRSA polymerase chain reaction (PCR) nasal swab in ventilator-associated pneumonia, lung abscess, and empyema. *Diagnostic Microbiology and Infectious Disease* 2023; **105(1)**, 115836.

[7] SP Bergin, TL Holland, VG Fowler and SYC Tong. Bacteremia, sepsis, and infective endocarditis associated with *Staphylococcus aureus*. *Current Topics in Microbiology and Immunology* 2017; **409**, 263-296.

[8] R Tabassum, S Kousar, G Mustafa, A Jamil and SA Attique. *In silico* method for the screening of phytochemicals against methicillin-resistant *Staphylococcus aureus*. *BioMed Research International* 2023; **2023(1)**, 5100400.

[9] M Fitranda, SIO Salasia, O Sianipar, DA Dewananda, AZ Arjana, F Aziz, M Wasissa, FB Lestari and CM Santosa. Methicillin-resistant *Staphylococcus aureus* isolates derived from humans and animals in Yogyakarta, Indonesia. *Veterinary World* 2023; **16(1)**, 239-245.

[10] Y Katayama, HZ Zhang and HF Chambers. PBP 2a mutations producing very-high-level resistance to beta-lactams. *Antimicrobial Agents and Chemotherapy* 2004; **48(2)**, 453-459.

[11] JM Intravia, MN Osterman and R Tosti. Antibiotic management and antibiotic resistance in hand infections. *Hand Clinics* 2020; **36(3)**, 301-305.

[12] R Sobral and A Tomasz. The staphylococcal cell wall. *Microbiology Spectrum* 2019. http://doi.org/10.1128/microbiolspec.gpp3-0068-2019.

[13] D Lim and NCJ Strynadka. Structural basis for the β lactam resistance of PBP2a from methicillin-resistant *Staphylococcus aureus*. *Nature Structural Biology* 2002; **9(11)**, 870-876.

[14] J Zhou, Z Feng, W Zhang and J Xu. Evaluation of the antimicrobial and cytotoxic potential of endophytic fungi extracts from mangrove plants *Rhizophora stylosa* and *R. mucronata*. *Scientific Reports* 2022; **12(1)**, 2733.

[15] KF Ghazawi, SA Fatani, SGA Mohamed, GA Mohamed and SRM Ibrahim. *Aspergillus nidulans*-Natural metabolites powerhouse: Structures, biosynthesis, bioactivities, and biotechnological potential. *Fermentation* 2023; **9(4)**, 325.

[16] J Kjer, A Debbab, AH Aly and P Proksch. Methods for isolation of marine-derived endophytic fungi and their bioactive secondary products. *Nature Protocols* 2010; **5(3)**, 479-490.

[17] A Windarsih, Suratno, HD Warmiko, AW Indrianingsih, A Rohman and YI Ulumuddin. Untargeted metabolomics and proteomics approach using liquid chromatography-Orbitrap high resolution mass spectrometry to detect pork adulteration in *Pangasius hypopthalmus* meat. *Food Chemistry* 2022; **386**, 132856.

[18] M Balouiri, M Sadiki and SK Ibnsouda. Methods for *in vitro* evaluating antimicrobial activity: A review. *Journal of Pharmaceutical Analysis* 2016; **6(2)**, 71-79.

[19] S Abraham, A Basukriadi, S Pawiroharsono and W Sjamsuridzal. Insecticidal activity of ethyl acetate extracts from culture filtrates of mangrove fungal endophytes. *Mycobiology* 2015; **43(2)**, 137-149.

[20] A Maurya, K Kalani, SC Verma, R Singh and A Srivastava. Vacuum liquid chromatography: Simple, efficient and versatile separation technique for natural products. *Organic &*

Medicinal Chemistry International Journal 2018; **7(2)**, 80-82.

[21] R Tautenhahn, C Böttcher and S Neumann. Highly sensitive feature detection for high resolution LC/MS. *BMC Bioinformatics* 2008; **9**, 504.

[22] E Chekmeneva, GDS Correia, M Gómez-Romero, J Stamler, Q Chan, P Elliott, JK Nicholson and E Holmes. Ultra-performance liquid chromatography-high-resolution mass spectrometry and direct infusion-high-resolution mass spectrometry for combined exploratory and targeted metabolic profiling of human urine. *Journal of Proteome Research* 2018; **17(10)**, 3492-3502.

[23] S Singha, V Gowda and MS Hedenqvist. Plant cuticle-inspired polyesters as promising green and sustainable polymer materials. *ACS Applied Polymer Materials* 2021; **3(8)**, 4088-4100.

[24] Y Wang, D Li, J Gao, X Li, R Zhang, X Jin, Z Hu, B Zheng, S Persson and P Chen. The 2'-O-methyladenosine nucleoside modification gene OsTRM13 positively regulates salt stress tolerance in rice. *Journal of Experimental Botany* 2017; **68(7)**, 1479-1491.

[25] J Das, R Kumar, SK Yadav and G Jha. Nicotinic acid catabolism modulates bacterial mycophagy in Burkholderia gladioli strain NGJ1. *Microbiology Spectrum* 2023; **11(3)**, e0445722.

[26] N Fujimori and H Ashihara. Adenine metabolism and the synthesis of purine alkaloids in flowers of *Camellia. Phytochemistry* 1990; **29(11)**, 3513-3516.

[27] A Turk, S Lee, SW Yeon, SH Ryu, YK Han, YJ Kim, SM Ko, BS Kim, BY Hwang, KY Lee and MK Lee. Adenosine deaminase inhibitory activity of medicinal plants: Boost the production of cordycepin in cordyceps militaris. *Antioxidants* 2023; **12(6)**, 1260.

[28] MK Arumugam, MC Paal, TMJ Donohue, M Ganesan, NA Osna and KK Kharbanda. Beneficial effects of betaine: A comprehensive review. *Biology* 2021; **10(6)**, 456.

[29] D Dobrijević, K Pastor, N Nastić, F Özogul, J Krulj, B Kokić, E Bartkiene, JM Rocha and J Kojić. Betaine as a functional ingredient: Metabolism, health-promoting attributes, food sources, applications and analysis methods. *Molecules* 2023; **28(12)**, 4824.

[30] W Wang, S Yamaguchi, M Koyama, S Tian, A Ino, K Miyatake and K Nakamura. LC-MS/MS analysis of choline compounds in Japanese-cultivated vegetables and fruits. *Foods* 2020; **9(8)**, 1029.

[31] C Akin-Osanaiye, A Gabriel and R Alebiosu. Characterization and antimicrobial screening of ethyl oleate isolated from *Phyllanthus Amarus* (Schum and Thonn). *Annuals of Biological Research* 2011; **2(2)**, 298-305.

[32] S Ramachandran, P Fontanille, A Pandey and C Larroche. Gluconic acid: Properties, applications and microbial production. *Food Technology & Biotechnology* 2006; **44(2)**, 185-195.

[33] A Durazzo, M Lucarini, A Nazhand, SB Souto, AM Silva, P Severino, EB Souto and A Santini. The nutraceutical value of carnitine and its use in dietary supplements. *Molecules* 2020; **25(9)**, 2127.

[34] ACMF Araújo, WMC Araújo, UML Marquez, R Akutsu and EY Nakano. Table of phenylalanine content of foods: Comparative analysis of data compiled in food composition tables. *JIMD Reports* 2017; **34**, 87-96.

[35] MR Hasan, MM Haque, MA Hoque, S Sultana, MM Rahman, MAA Shaikh and MKU Sarker. Antioxidant activity study and GC-MS profiling of *Camellia sinensis* Linn. *Heliyon* 2024; **10(1)**, e23514.

[36] E Okuyama, T Hasegawa, T Matsushita, H Fujimoto, M Ishibashi and M Yamazaki. Analgesic components of saposhnikovia root (Saposhnikovia divaricata). *Chemical & Pharmaceutical Bulletin* 2001; **49(2)**, 154-160.

[37] G Chen, M Zhu and M Guo. Research advances in traditional and modern use of Nelumbo nucifera: Phytochemicals, health promoting activities and beyond. *Critical Reviews in Food Science and Nutrition* 2019; **59(S1)**, S189-S209.

[38] PW Harlina, V Maritha, R Shahzad, M Rafi, F Geng, I Musfiroh, M Muchtaridi, R Wahab, AA Al-Khedhairy, S Koerniati and NN Amalina. Comprehensive profiling and authentication of porcine, bovine, and goat bone gelatins through UHPLC-HRMS metabolomics and chemometric strategies. *LWT* 2024; **205**, 116529.

[39] CY Ma, WK Liu and CT Che. Lignanamides and nonalkaloidal components of Hyoscyamus niger seeds. *Journal of Natural Products* 2002; **65(2)**, 206-209.

[40] D Wang, TJ Girard, TP Kasten, RM LaChance, MA Miller-Wideman and RC Durley. Inhibitory activity of unsaturated fatty acids and anacardic acids toward soluble tissue factor-factor VIIa complex. *Journal of Natural Products* 1998; **61(11)**, 1352-1355.

[41] RM Munavu. Fatty acid composition of seed kernel oil of *Calodendrum capense* (L.f.) Thunb. *Journal of the American Oil Chemists Society* 1983; **60(9)**, 1653-1653.

[42] K Machida, LS Trifonov, WA Ayer, ZX Lu, A Laroche, HC Huang, KJ Cheng and JL Zantige. 3(2H)-Benzofuranones and chromanes from liquid cultures of the mycoparasitic fungus *Coniothyrium minitans*. *Phytochemistry* 2001; **58(1)**, 173-177.

[43] M Isaka, P Chinthanom, S Kongthong, S Supothina and P Ittiworapong. Hamigeromycins C-G, 14-membered macrolides from the fungus *Hamigera avellanea* BCC 17816. *Tetrahedron* 2010; **66(4)**, 955-961.

[44] K Fidyt, A Fiedorowicz, L Strządała and A Szumny. β-caryophyllene and β-caryophyllene oxide-natural compounds of anticancer and analgesic properties. *Cancer Medicine* 2016; **5(10)**, 3007-3017.

[45] C Delgado, G Mendez-Callejas and C Celis. Caryophyllene oxide, the active compound isolated from leaves of *Hymenaea courbaril* L.(Fabaceae) with antiproliferative and apoptotic effects on PC-3 androgen-independent prostate cancer cell line. *Molecules* 2021; **26(20)**, 6142.

[46] X Liu and W Quan. Progress on the synthesis pathways and pharmacological effects of naturally occurring pyrazines. *Molecules* 2024; **29(15)**, 3597.

[47] K Mogi, Y Koya, M Yoshihara, M Sugiyama, R Miki, E Miyamoto, H Fujimoto, K Kitami, S Iyoshi, S Tano, K Uno, S Tamauchi, A Yokoi, Y Shimizu, Y Ikeda, N Yoshikawa, K Niimi, Y Yamakita, H Tomita, K Shibata, A Nawa, Y Tomoda and H Kajiyama. 9-oxo-ODAs suppresses the proliferation of human cervical cancer cells through the inhibition of CDKs and HPV oncoproteins. *Scientific Reports* 2023; **13(1)**, 19208.

[48] ZP Yu, C An, Y Yao, CY Wang, Z Sun, C Cui, L Liu and SS Gao. A combined strategy for the overproduction of complex ergot alkaloid agroclavine. *Synthetic and Systems Biotechnology* 2022; **7(4)**, 1126-1132.

[49] MM Gutiérrez-Pacheco, H Torres-Moreno, ML Flores-Lopez, NV Guadarrama, JF Ayala-Zavala, LA Ortega-Ramírez and JC López-Romero. Mechanisms and applications of citral's antimicrobial properties in food preservation and pharmaceuticals formulations. *Antibiotics* 2023; **12(11)**, 1608.

[50] SA Ashraf, AEO Elkhalifa, AJ Siddiqui, M Patel, AM Awadelkareem, M Snoussi, MS Ashraf, M Adnan and S Hadi. Cordycepin for health and wellbeing: A potent bioactive metabolite of an entomopathogenic medicinal fungus Cordyceps with its nutraceutical and therapeutic potential. *Molecules* 2020; **25(12)**, 2735.

[51] K Naumoska, U Jug, V Metličar and I Vovk. Oleamide, a bioactive compound, unwittingly introduced into the human body through some plastic food/beverages and medicine containers. *Foods* 2020; **9(5)**, 549.

[52] KK Yadav, N Gupta, S Prasad, LC Malav, JK Bhutto, A Ahmad, A Gacem, BH Jeon, AM Fallatah, BH Asghar, MMS Cabral-Pinto, NS Awwad, OKR Alharbi, M Alam and S Chaiprapat. An eco-sustainable approach towards heavy metals remediation by mangroves from the coastal environment: A critical review. *Marine Pollution Bulletin* 2023; **188**, 114569.

[53] MUE Sanam, AIR Detha and NK Rohi. Detection of antibacterial activity of lactic acid bacteria, isolated from Sumba mare's milk, against Bacillus cereus, Staphylococcus aureus, and Escherichia coli. *Journal of Advanced Veterinary and Animal Research* 2022; **9(1)**, 53-58.

[54] V Jeyanthi and P Velusamy. Anti-methicillin resistant *Staphylococcus aureus* compound isolation from halophilic *Bacillus amyloliquefaciens* MHB1 and determination of its mode of action using electron microscope and

flow cytometry analysis. *Indian Journal of Microbiology* 2016; **56(2)**, 148-157.

[55] MAW Shalaby, EME Dokla, RAT Serya and KAM Abouzid. Penicillin binding protein 2a: An overview and a medicinal chemistry perspective. *European Journal of Medicinal Chemistry* 2020; **199**, 112312.

[56] B Morak-Młodawska, M Jeleń, E Martula and R Korlacki. Study of lipophilicity and ADME properties of 1,9-diazaphenothiazines with anticancer action. *International Journal of Molecular Sciences* 2023; **24(8)**, 6970.

[57] D Gadaleta, K Vuković, C Toma, GJ Lavado, AL Karmaus, K Mansouri, NC Kleinstreuer, E Benfenati and A Roncaglioni. SAR and QSAR modeling of a large collection of LD_{50} rat acute oral toxicity data. *Journal of Cheminformatics* 2019; **11(1)**, 58.

[58] J Raj, M Chandra, TD Dogra, M Pahuja and A Raina. Determination of median lethal dose of combination of endosulfan and cypermethrin in wistar rat. *Toxicology International* 2013; **20(1)**, 1-5.

[59] M Masumi, F Noormohammadi, F Kianisaba, F Nouri, M Taheri and A Taherkhani. Methicillin-resistant *Staphylococcus aureus*: Docking-based virtual screening and molecular dynamics simulations to identify potential penicillin-binding protein 2a inhibitors from natural flavonoids. *International Journal of Microbiology* 2022; **2022**, 9130700.

[60] SJ Uddin, J Bettadapura, P Guillon, ID Grice, S Mahalingam and E Tiralongo. *In-vitro* antiviral activity of a novel phthalic acid ester derivative isolated from the Bangladeshi mangrove fern *Acrostichum aureum*. *Journal of Antivirals & Antiretrovirals* 2013; **5(6)**, 139-144.

[61] ALDS Pontes, VC Mesquita, FDO Chaves, AJRD Silva, MAC Kaplan and CE Fingolo. Phthalates in *Avicennia schaueriana*, a mangrove species, in the State Biological Reserve, Guaratiba, RJ, Brazil. *Environmental Advances* 2020; **2**, 100015.

[62] CP Victório, MSD Santos and NK Simas. Phthalates: Environmental pollutants detected in leaf epicuticular wax of *Avicennia schaueriana* and *Rhizophora mangle* from a mangrove ecosystem. *International Journal of Environmental Studies* 2022; **79(1)**, 114-123.

[63] HJ Kwon, H Ahn, BS Kim, SS Kang and KG Lee. Anti-bacterial and anti-inflammatory activities of lactic acid bacteria-bioconversioned indica rice (*Oryza sativa* L.) extract. *Chemical and Biological Technologies in Agriculture* 2022; **9**, 44.

[64] SB Izzati, SIN Anidah and AA Yusmur. Antibacterial activity profile of mangrove endophytic fungi isolated from berau regency, Indonesia. *Indonesian Journal of Biotechnology & Bioscience* 2022; **9(1)**, 86-99.

[65] D Kusumah, M Wakui, M Murakami, X Xie, K Yukihito and I Maeda. Linoleic acid, α-linolenic acid, and monolinolenins as antibacterial substances in the heat-processed soybean fermented with *Rhizopus oligosporus*. *Bioscience, Biotechnology, and Biochemistry* 2020; **84(6)**, 1285-1290.

[66] BK Yoon, JA Jackman, ER Valle-González and NJ Cho. Antibacterial free fatty acids and monoglycerides: Biological activities, experimental testing, and therapeutic applications. *International Journal of Molecular Sciences* 2018; **19(4)**, 1114.

Supplementary material

Table S1 Metabolites of crude ethyl acetate from *E. nidulans* identified by LC-HRMS.

No	Name	Formula	Annot. Source: mzCloud Search	Annot. DeltaMass [ppm]	mzCloud Best Match
1	(-)-Caryophyllene oxide	$C_{15}H_{24}O$	Full match	-1.21	90.2
2	1,2,3,4-Tetramethyl-1,3-cyclopentadiene	C_9H_{14}	Full match	0.02	92.6
3	16-Hydroxyhexadecanoic acid	$C_{16}H_{32}O_3$	Full match	0.36	91
4	1-Linoleoyl glycerol	$C_{21}H_{38}O_4$	Full match	-2.64	98.5
5	2-(Acetylamino)hexanoic acid	$C_8H_{15}NO_3$	Full match	-4.41	99.7
6	2,3,5,6-Tetramethylpyrazine	$C_8H_{12}N_2$	Full match	-0.63	99.9
7	2-Hydroxyquinoline	C_9H_7NO	Full match	-0.4	91.4
8	2-Naphthylamine	$C_{10}H_9N$	Full match	-0.61	96.2
9	2'-O-Methyladenosine	$C_{11}H_{15}N_5O_4$	Full match	-0.4	99.4
10	4-Methyl-5-thiazoleethanol	C_6H_9NOS	Full match	0.1	98.3
11	6-(4-methoxybenzyl)-3-methyl-5,6,7,8-tetrahydroquinoline	$C_{18}H_{21}NO$	Full match	-0.59	94.9
12	6-Hydroxynicotinic acid	$C_6H_5NO_3$	Full match	-0.62	95.6
13	9(Z),11(E),13(E)-Octadecatrienoic Acid methyl ester	$C_{19}H_{32}O_2$	Full match	-2.12	97.8
14	9-Oxo-10(E),12(E)-octadecadienoic acid	$C1_8H_{30}O_3$	Full match	-1.51	96.5
15	Adenine	$C_5H_5N_5$	Full match	-1.5	99.3
16	Adenosine	$C_{10}H_{13}N_5O_4$	Full match	-1.47	99.9
17	Agroclavine	$C_{16}H_{18}N_2$	Full match	-0.81	97.4
18	Auramine	$C_{17}H_{21}N_3$	Full match	2.26	91.2
19	Betaine	$C_5H_{11}NO_2$	Full match	-0.36	94.8
20	Bis(3,5,5-trimethylhexyl) phthalate	$C_{26}H_{42}O_4$	Full match	-2.76	98.3
21	Bis(4-ethylbenzylidene)sorbitol	$C_{24}H_{30}O_6$	Full match	-0.32	99.9
22	Bis(7-methyloctyl) adipate	$C_{24}H_{46}O_4$	Full match	-3.81	95.9
23	Choline	$C_5H_{13}NO$	Full match	1.89	93.4
24	cis-12-Octadecenoic acid methyl ester	C19 H36 O2	Full match	-2.26	96.9
25	Citral	$C_{10}H_{16}O$	Full match	-0.54	90.8
26	Cordycepin	$C_{10}H_{13}N_5O_3$	Full match	-1.7	99.9
27	Dextromethorphan	$C_{18}H_{25}NO$	Full match	-0.76	98.8
28	Ethyl oleate	$C_{20}H_{38}O_2$	Full match	-2.53	98.9
29	Gluconic acid	$C_6H_{12}O_7$	Full match	-2.96	97.3
30	Hypoxanthine	$C_5H_4N_4O$	Full match	-2.66	99.5
31	L(-)-Carnitine	$C_7H_{15}NO_3$	Full match	-0.55	98.5
32	L-Phenylalanine	$C_9H_{11}NO_2$	Full match	0.57	99.1
33	Methyl palmitate	$C_{17}H_{34}O_2$	Full match	-0.69	96.6
34	Mono(2-ethylhexyl) phthalate (MEHP)	$C_{16}H_{22}O_4$	Full match	-0.54	99.7
35	Monoolein	$C_{21}H_{40}O_4$	Full match	-2.51	98.5
36	N,N-Diethyldodecanamide	$C_{16}H_{33}NO$	Full match	-1.32	97.9
37	Nicotinic acid	$C_6H_5NO_2$	Full match	-0.54	99.7
38	NP-007065	$C_8H_{10}O_3$	Full match	-1.31	94.3
39	NP-019401	$C_{11}H_{15}NO_2$	Full match	-0.54	97.2
40	NP-021797	$C_{12}H_{22}O_3$	Full match	-2.23	92.8

No	Name	Formula	Annot. Source: mzCloud Search	Annot. DeltaMass [ppm]	mzCloud Best Match
41	Oleamide	$C_{18}H_{35}NO$	Full match	-1.65	99.1
42	Oxepanone	$C_6H_{10}O_2$	Full match	1.06	90.8
43	Palmitic Acid	$C_{16}H_{32}O_2$	Full match	-0.63	99.6
44	Propranolol	$C_{16}H_{21}NO_2$	Full match	-0.06	96.9
45	Stearamide	$C_{18}H_{37}NO$	Full match	-1.26	99.3
46	Uracil	$C_4H_4N_2O_2$	Full match	0.34	94.4
47	α-Linolenic acid	$C_{18}H_{30}O_2$	Full match	-1.59	95.7

Table S2 Zona of inhibition of crude extract and ethyl acetate fractions, positive, negative controls using agar disc diffusion method against MRSA bacteria.

Name	Inhibition Zone -1	Inhibition zone -2	Average	SD
c	7.154	7.461	7.31	0.217
4	9.57	9.679	9.62	0.077
6	8.505	8.877	8.69	0.263
7	8.2195	7.797	8.01	0.299
8	7.452	7.26	7.36	0.136
9	7.499	7.731	7.62	0.164
kontrol +	19.3915	19.821	19.61	0.304
kontrol -	-	-	0	0

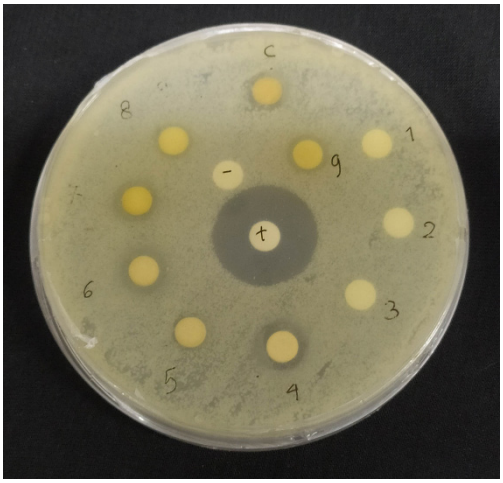

(1)

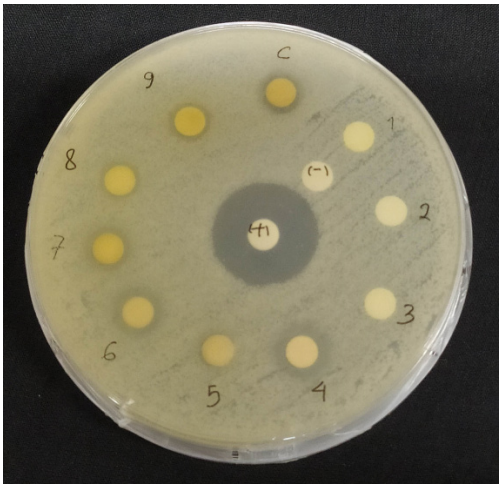

(2)

Table S3 Redocking native ligan.

Name	Rerank Score	RMSD	H-Bond
[00]PNM_708 [B]	-102.32	6.56398	-10.406
[01]PNM_708 [B]	-98.0868	6.44502	-9.61451
[02]PNM_708 [B]	-86.8684	6.21571	-10.7001
[04]PNM_708 [B]	-88.0493	4.26014	-1.93897
[03]PNM_708 [B]	-87.0279	0.93474	-6.77561

Name	Rerank Score	RMSD	H-Bond
[00]PNM_708 [B]	-108.358	6.18759	-11.2522
[01]PNM_708 [B]	-87.944	1.06168	-6.70148
[03]PNM_708 [B]	-91.4791	8.53273	-11.1226
[02]PNM_708 [B]	-95.7414	6.56903	-5.55215
[04]PNM_708 [B]	-86.2791	4.0038	-5.4055

Name	Rerank Score	RMSD	H-Bond
[00]PNM_708 [B]	-78.2458	6.35459	-5.35443
[02]PNM_708 [B]	-94.3465	6.77375	-9.08175
[03]PNM_708 [B]	-81.9836	0.889592	-8.59979
[01]PNM_708 [B]	-74.1953	6.81046	-4.4656
[04]PNM_708 [B]	-82.5967	2.89391	-3.82704

Tabel S4 Ligand-protein binding affinity (rerank score) from highest to lowest of 47 compounds and their pose.

No	Name	Rerank Score	H-Bond
1	[00]Bis(3,5,5-trimethylhexyl) phthalate	-100.88	-5.9834
2	[03]1-Linoleoyl glycerol	-99.7437	-3.6108
3	[01]9-Oxo-10(E)12(E)-octadecadienoic acid	-99.4385	-9.04193
4	[02]Monoolein	-96.5963	-6.31963
5	[03]Bis(355-trimethylhexyl) phthalate	-96.4638	-3.79345
6	[01]1-Linoleoyl glycerol	-94.7042	-7.41909
7	[00]Monoolein	-94.0065	-6.63761
8	[00]9(Z)11(E)13(E)-Octadecatrienoic Acid methyl ester	-93.7813	-4.43592
9	[00]1-Linoleoyl glycerol	-93.3303	-12.8115
10	[00]Bis(7-methyloctyl) adipate	-93.0731	-2.44621
11	[00]Bis(4-ethylbenzylidene)sorbitol	-93.0372	-7.45552
12	[00]a-Linolenic acid	-92.6499	-2.5
13	[00]9-Oxo-10(E)12(E)-octadecadienoic acid	-92.2386	-0.460225
14	[04]1-Linoleoyl glycerol	-92.0877	-4.40175
15	[03]a-Linolenic acid	-91.6079	-5
16	[03]Bis(4-ethylbenzylidene)sorbitol	-90.8891	-5.53547
17	[03]Monoolein	-90.7249	-7.03708
18	[02]Bis(355-trimethylhexyl) phthalate	-89.7309	-5.64308
19	[02]a-Linolenic acid	-89.3753	-2.86418
20	[00]Oleamide	-89.305	-2.42902

No	Name	Rerank Score	H-Bond
21	[02]Oleamide	-88.7873	0
22	[01]a-Linolenic acid	-88.5555	-2.82333
23	[02]9-Oxo-10(E)12(E)-octadecadienoic acid	-88.2999	-5.56846
24	[03]cis-12-Octadecenoic acid methyl ester	-87.96	-1.47976
25	[02]cis-12-Octadecenoic acid methyl ester	-87.6737	0
26	[01]Oleamide	-87.5125	-5.61994
27	[01]Mono(2-ethylhexyl) phthalate (MEHP)	-86.6211	-7.34391
28	[02]16-Hydroxyhexadecanoic acid	-86.2216	-8.2355
29	[04]9-Oxo-10(E)12(E)-octadecadienoic acid	-86.0176	-4.09813
30	[04]Mono(2-ethylhexyl) phthalate (MEHP)	-85.9936	-7.87754
31	[02]9(Z)11(E)13(E)-Octadecatrienoic Acid methyl ester	-85.9901	-1.25288
32	[01]Monoolein	-85.8426	-3.54845
33	[03]Mono(2-ethylhexyl) phthalate (MEHP)	-85.5735	-7.50277
34	[03]Bis(7-methyloctyl) adipate	-85.3315	1.34351
35	[04]9(Z)11(E)13(E)-Octadecatrienoic Acid methyl ester	-85.2081	0
36	[04]Methyl palmitate	-84.6685	0
37	[03]9-Oxo-10(E)12(E)-octadecadienoic acid	-84.6489	-5.1998
38	[01]cis-12-Octadecenoic acid methyl ester	-84.5797	-1.84688
39	[02]Bis(7-methyloctyl) adipate	-84.5571	-4.16694
40	[04]Monoolein	-84.4394	-3.38436
41	[01]Bis(4-ethylbenzylidene)sorbitol	-84.1944	-6.79652
42	[02]Mono(2-ethylhexyl) phthalate (MEHP)	-83.9103	-8.83675
43	[04]16-Hydroxyhexadecanoic acid	-83.4949	-2.89404
44	[02]1-Linoleoyl glycerol	-83.4097	-7.67241
45	[00]Mono(2-ethylhexyl) phthalate (MEHP)	-83.1301	-8.286
46	[00]16-Hydroxyhexadecanoic acid	-82.6508	-7.79439
47	[04]cis-12-Octadecenoic acid methyl ester	-82.4798	-2.35745
48	[00]Palmitic Acid	-82.4686	-5.09866
49	[04]Bis(4-ethylbenzylidene)sorbitol	-81.7662	-6.35049
50	[02]Methyl palmitate	-81.0995	-4.90473
51	[01]2'-O-Methyladenosine	-80.7802	-14.4295
52	[00]Cordycepin	-80.1664	-5.16197
53	[01]Bis(355-trimethylhexyl) phthalate	-80.0928	-1.02612
54	[04]Oleamide	-80.073	-4.45956
55	[00]Methyl palmitate	-79.9853	-2.16027
56	[03]16-Hydroxyhexadecanoic acid	-79.7709	-5.31181
57	[02]Stearamide	-79.7156	-1.38285
58	[04]Bis(7-methyloctyl) adipate	-79.654	-1.4244
59	[04]Stearamide	-79.4456	-2.21354
60	[01]9(Z)11(E)13(E)-Octadecatrienoic Acid methyl ester	-79.0519	-3.69334
61	[01]16-Hydroxyhexadecanoic acid	-79.0214	-5.51054
62	[01]Auramine	-78.9094	-3.59893
63	[03]2'-O-Methyladenosine	-78.6247	-7.05925
64	[01]Palmitic Acid	-78.5365	-2.42149
65	[00]Propranolol	-77.9459	-5.89863

No	Name	Rerank Score	H-Bond
66	[02]Adenosine	-77.7075	-5.8842
67	[00]Adenosine	-77.6757	-10.2468
68	[02]Cordycepin	-77.6161	-14.9723
69	[01]Bis(7-methyloctyl) adipate	-77.4278	-2.40154
70	[00]Auramine	-77.2345	-3.56153
71	[00]NP-021797	-75.9999	-5.80763
72	[00]Stearamide	-75.8708	-2.5
73	[00]NN-Diethyldodecanamide	-75.7446	0
74	[02]NP-021797	-75.1767	-4.93717
75	[02]Palmitic Acid	-74.4298	-2.92471
76	[03]Methyl palmitate	-74.3445	-6.40543
77	[03]NN-Diethyldodecanamide	-74.054	-0.291395
78	[03]Oleamide	-73.041	-1.74009
79	[03]Adenosine	-72.4303	-13.0106
80	[00]2'-O-Methyladenosine	-72.1714	-21.4538
81	[02]Auramine	-71.7912	-0.225977
82	[02]NN-Diethyldodecanamide	-71.7443	-0.737518
83	[04]NN-Diethyldodecanamide	-71.3984	0
84	[03]Stearamide	-71.3001	-1.23356
85	[04]Palmitic Acid	-71.0646	-2.5
86	[04]Propranolol	-70.633	-4.50385
87	[01]NP-021797	-70.6187	-6.76635
88	[03]Auramine	-68.9377	-0.428459
89	[04]NP-021797	-68.9141	-7.52115
90	[04]Cordycepin	-68.8673	-10.5802
91	[03]NP-021797	-68.7871	-9.76148
92	[00]6-(4-methoxybenzyl)-3-methyl-5678-tetrahydroquinoline	-68.5458	-1.11333
93	[01]Methyl palmitate	-68.3607	0
94	[00]cis-12-Octadecenoic acid methyl ester	-68.1318	-1.31298
95	[02]4-Methyl-5-thiazoleethanol	-67.9104	-10.8236
96	[03]Propranolol	-67.0041	-5.31056
97	[01]6-(4-methoxybenzyl)-3-methyl-5678-tetrahydroquinoline	-66.8426	-1.43685
98	[01]Propranolol	-66.3423	-3.24448
99	[01](-)-Caryophyllene oxide	-66.2863	-1.62519
100	[00]NP-019401	-66.2743	-6.97847
101	[03]Palmitic Acid	-65.9563	-3.39609
102	[02]Agroclavine	-65.7931	-0.647608
103	[01]Agroclavine	-64.9453	0
104	[01]NN-Diethyldodecanamide	-64.9075	0
105	[01]2-(Acetylamino)hexanoic acid	-64.5354	-4.91175
106	[01]Gluconic acid	-64.4708	-14.9517
107	[00]2-(Acetylamino)hexanoic acid	-64.2691	-8.89995
108	[00]Gluconic acid	-62.9634	-16.6648
109	[01]4-Methyl-5-thiazoleethanol	-62.615	-8.56635
110	[01]Adenosine	-62.3446	-10.7287

No	Name	Rerank Score	H-Bond
111	[00]Citral	-61.612	-1.33996
112	[03]4-Methyl-5-thiazoleethanol	-61.3265	-9.21041
113	[01]Citral	-61.1732	-0.130567
114	[03]Citral	-60.6979	-1.87805
115	[00](-)-Caryophyllene oxide	-60.471	0
116	[01]L(-)-Carnitine	-60.0031	-4.24711
117	[02]2-(Acetylamino)hexanoic acid	-59.8954	-6.04969
118	[02](-)-Caryophyllene oxide	-59.7307	0
119	[00]L-Phenylalanine	-59.5214	-10.4432
120	[01]Cordycepin	-59.2273	-17.1433
121	[04]2-(Acetylamino)hexanoic acid	-59.0124	-7.1669
122	[00]4-Methyl-5-thiazoleethanol	-58.9946	-7.18977
123	[02]Citral	-58.9504	-1.305
124	[03]NP-019401	-58.7595	-8.67068
125	[02]Gluconic acid	-58.563	-15.5543
126	[02]L(-)-Carnitine	-58.2073	-4.78643
127	[04]4-Methyl-5-thiazoleethanol	-58.1602	-8.18581
128	[03]Gluconic acid	-57.9537	-11.6162
129	[01]NP-019401	-57.8171	-4.40738
130	[02]NP-019401	-57.525	-8.61029
131	[04]L(-)-Carnitine	-57.4778	-1.59815
132	[02]Bis(4-ethylbenzylidene)sorbitol	-57.3664	-6.38053
133	[02]Propranolol	-56.8982	-6.08721
134	[01]Stearamide	-56.7575	-2.7668
135	[03]L(-)-Carnitine	-55.5743	-4.74109
136	[01]L-Phenylalanine	-55.5048	-9.1854
137	[04]Gluconic acid	-55.4855	-12.9021
138	[03]Cordycepin	-53.4567	-12.029
139	[03]2-(Acetylamino)hexanoic acid	-53.3759	-4.77607
140	[02]6-(4-methoxybenzyl)-3-methyl-5678-tetrahydroquinoline	-52.9569	-2.83364
141	[04]L-Phenylalanine	-51.4924	-7.94145
142	[02]L-Phenylalanine	-51.4825	-10.1581
143	[04]Citral	-49.7148	-0.138216
144	[03]6-(4-methoxybenzyl)-3-methyl-5678-tetrahydroquinoline	-49.5182	0
145	[00]NP-007065	-49.5074	-5.45804
146	[03]NP-007065	-49.4535	-6.7743
147	[01]NP-007065	-48.9114	-5.35584
148	[02]NP-007065	-48.6819	-7.66776
149	[00]6-Hydroxynicotinic acid	-48.0573	-6.78948
150	[01]6-Hydroxynicotinic acid	-46.9929	-7.6213
151	[00]1234-Tetramethyl-13-cyclopentadiene	-46.9778	0
152	[04]NP-007065	-46.6884	-3.59256
153	[02]1234-Tetramethyl-13-cyclopentadiene	-46.5417	0
154	[02]6-Hydroxynicotinic acid	-46.442	-8.05999
155	[04]1234-Tetramethyl-13-cyclopentadiene	-46.4225	0

No	Name	Rerank Score	H-Bond
156	[01]1234-Tetramethyl-13-cyclopentadiene	-46.3585	0
157	[02]2-Naphthylamine	-46.3461	-4.53024
158	[04]2-Naphthylamine	-45.626	-1.75106
159	[04]2-Hydroxyquinoline	-45.4538	-2.63972
160	[00]2-Naphthylamine	-45.213	-1.79219
161	[01]2-Naphthylamine	-45.2077	-2.50378
162	[03]1234-Tetramethyl-13-cyclopentadiene	-45.0942	0
163	[03]2-Naphthylamine	-44.9473	-2.51016
164	[03]2-Hydroxyquinoline	-44.6256	-2.43322
165	[04]Agroclavine	-44.5355	-0.988132
166	[04]6-Hydroxynicotinic acid	-44.1231	-2.90546
167	[03]L-Phenylalanine	-44.0846	-6.47747
168	[02]Adenine	-43.8122	-10.4878
169	[01]2-Hydroxyquinoline	-43.5342	0
170	[03]Nicotinic acid	-43.4458	-7.18574
171	[03](-)-Caryophyllene oxide	-43.4414	0
172	[00]Hypoxanthine	-43.305	-5.47611
173	[01]Betaine	-43.2409	-2.83382
174	[01]Adenine	-42.9816	-9.3729
175	[00]Nicotinic acid	-42.8075	-8.71067
176	[04]Adenosine	-42.7887	-10.6034
177	[03]Adenine	-42.7342	-7.07846
178	[02]2-Hydroxyquinoline	-42.7156	-1.20905
179	[02]Betaine	-42.4616	-5.06215
180	[00]L(-)-Carnitine	-41.9847	-5.36429
181	[04]Betaine	-41.8386	-4.70698
182	[04]Adenine	-41.7761	-10.4152
183	[03]6-Hydroxynicotinic acid	-41.7721	-4.84281
184	[04]Nicotinic acid	-41.6652	-4.70666
185	[03]Betaine	-41.4843	-2.1685
186	[00]2356-Tetramethylpyrazine	-41.4257	-0.398587
187	[03]Agroclavine	-41.3999	0
188	[01]2356-Tetramethylpyrazine	-41.2221	-0.33536
189	[01]Nicotinic acid	-41.1049	-6.66666
190	[02]Nicotinic acid	-40.6379	-2.69798
191	[03]Hypoxanthine	-40.1052	-7.61126
192	[02]Oxepanone	-39.6532	-1.22822
193	[00]2-Hydroxyquinoline	-39.2104	-3.80321
194	[03]Oxepanone	-38.6155	-5.06897
195	[02]2356-Tetramethylpyrazine	-38.5653	0
196	[03]Choline	-38.3992	-2.49919
197	[04]Hypoxanthine	-38.381	-5.90778
198	[04]Choline	-38.2701	-2.79756
199	[04]2'-O-Methyladenosine	-38.167	-12.3621
200	[04]a-Linolenic acid	-38.1488	-3.90267

No	Name	Rerank Score	H-Bond
201	[02]Hypoxanthine	-38.0143	-5.83957
202	[01]Choline	-37.3559	-4.94612
203	[01]Hypoxanthine	-37.2158	-5.15982
204	[04]Oxepanone	-37.0884	-3.63352
205	[00]Choline	-36.3164	-2.5
206	[00]uracil	-35.9155	-4.02268
207	[02]uracil	-35.2422	-4.87495
208	[00]Adenine	-33.9612	-5.31285
209	[04]uracil	-33.4157	-4.31486
210	[02]Choline	-32.4742	-5.75638
211	[03]uracil	-31.8872	-6.05656
212	[01]uracil	-31.7142	-4.13358
213	[00]Betaine	-31.3708	-3.69156
214	[00]Agroclavine	-29.6262	0
215	[04]Bis(355-trimethylhexyl) phthalate	-29.1524	0
216	[03]9(Z)11(E)13(E)-Octadecatrienoic Acid methyl ester	-26.3487	-1.77128
217	[00]Oxepanone	-26.0676	-0.479393
218	[01]Oxepanone	-22.3825	-2.90206
219	[04]NP-019401	-14.8398	-8.14417
220	[04](-)-Caryophyllene oxide	-11.0443	-0.841496
221	[04]6-(4-methoxybenzyl)-3-methyl-5678-tetrahydroquinoline	-8.68266	-0.361715
222	[02]2'-O-Methyladenosine	-1.02183	-18.6325